J. Environ. Nanotechnol.
Volume 3, No.4 (2014) pp. 01-12
ISSN (Print): 2279-0748
ISSN (Online): 2319-5541
doi: 10.13074/jent.2015.03.143088

Synthesis, Characterisation and Computational Investigation of 2-[(4'-methylbenzylidene)amino]phenol

S. Anbuselvi[1*], V. Jayamani[2], R. Mathammal[3]

[1*,2]*Department of Chemistry, Sri Sarada College for Women (Autonomous), Salem, TN, India*
[3]*Department of physics, Sri Sarada College for Women (Autonomous,) Salem, TN, India*

Received:08.07.2014 Accepted:10.11.2014

Abstract

A theoretical study on molecular, electronic, vibrational, NMR, NBO, HOMO and LUMO analysis of 2-[(4'-Methylbenzylidene)amino]phenol .Also experimentally observed and theoretical IR data of the title compound are compared. The FT-IR spectra of the title compound are recorded in solid phase. The structural and vibrational spectroscopic analysis of the title compound was carried out by using density functional B3LYP method with the LanL2DZ basis set. The NMR spectroscopic analysis of the compound was carried out by using density functional B3LYP method with the 6-311+ G(d, p) basis set. The theoretical electronic absorption spectra have been calculated by using TD-DFT/ B3LYP method. Comparison of simulated vibrational spectra with the experimental spectra provides important information about the ability of computational method to describe the vibrational modes. The electronic dipole moment (μ_{tot}), molecular polarizability (α_{tot}), anisotropy of polarizability ($\Delta\alpha$) and the molecular first order hyper polarizability (β_{tot}) of the title compound are also computed. The influence of the title compound on the inhibition of corrosion of the metal surfaces are studied by density functional theory at the B3LYP/ LanL2DZ level.

Keywords: *2-[(4'-Methylbenzylidene)amino]phenol; DFT; FT-IR; Molecular orbital; NBO; NMR spectra.*

1. INTRODUCTION

Schiff's bases have been used in different areas such as electrochemistry, bioinorganic catalysis, metallic deactivators, separation process, environmental chemistry and pharmaceutical, dye, plastic industries as well as in the field of liquid – crystal technology (Shemirani *et al*.2004; Gupta *et al*. 2006; Nishinaga *et al*. 1988) Several Schiff bases possess anti-inflammatory (Dhar *et al*. 1982), radical scavenging (Hadjipavlu, 1998), analgesic(De and Ramasarma, 1999) anti-oxidative action and antiulcer activity (Luo *et al*. 2003).

DFT methods (Parr and Yang, 1989) have become a powerful tool for the investigation of molecular structure and spectral character. Furthermore the Density function theory (DFT) B3LYP/ LanL2DZ method was employed to investigate the second-order nonlinear optical (NLO) properties and inhibitor efficiency of Schiff base compounds. Organic compounds containing -CH=N groups have been foundto act as effective corrosion inhibitors for copper and its alloys in different corrosive media (Kertit *et al.* 1996; 1998; Yan *et al.* 2000; Essoufi *et al*. 2000; Zucchi *et al*. 1996). Natural bond orbitals depict the Lewis-like molecular bonding pattern of electrons as a set of optimally condensed and ortho-normal localized few-center orbital's (Sastri and Perumareddi, 1997). NBO analysis has been performed on the 2MBAP at the DFT level in order to elucidate the intramolecular,re-hybridization and delocalization of electron density within the molecule.

***S. Anbuselvi** Tel.no: +919994326374*
E-mail: selvisarachem@yahoo.com

2.EXPERIMENTAL DETAILS

2.1 Synthesis

Commercially available AR grade p-tolualdehyde, 2-aminophenol and ethanol were used without further purification to synthesize the 2MBAP by condensation method. Mixture of p-tolualdehyde (1 mmol), 2-aminophenol (1 mmol) and alcohol (20 mL) was heated under reflux for 5 h, cooled and

then poured into crushed ice and the yellow solid 2MBAP that separate out was collected by filtration, washed with water and dried. Crystallization was done from ethanol. Purity of the compound was checked by thin layer chromatography.

Colour : Yellow Yield: 1.9 g

IR measurement

The FT-IR spectrum of the synthesized material was recorded in the wave number range 400-4000 cm^{-1} by KBr pellet technique (Thermo Nicolet avatar 370 DTGS FT-IR spectrometer).

UV measurement

The UV spectrum of the synthesized material was recorded using TU-1901 V-VIS spectrophotometer.

3. THEORETICAL METHODOLOGY

DFT calculations were carried out using the Gaussian 09 program package. Initial geometry generated from standard geometrical parameters was minimized without any constant in the potential energy surface at B3LYP level adopting the standard lanl2dz basis set. The NMR spectroscopic analysis of the compound was carried out by using density functional B3LYP method with the 6-311+ G(d ,p) basis set. The 6-311+ G(d, p) basis set was chosen as a compromise between accuracy and applicability to large molecules.

All calculations, which include geometry optimizations, energies, reduced masses, electronic, vibrational and NMR spectra were performed on isolated system using the Backe's three parameter B3LYP exchange correlation method. Finally, the calculated normal mode vibrational frequencies provide thermodynamic properties also through the principle of statistical mechanics.By combining the results of the GAUSSVIEW program with symmetry considerations, vibrational frequencies assignments were made with a high degree of accuracy. For each donor (i) and acceptor (j), the stabilization energy E(2) associated with the delocalization i→ j is estimated as:

$$E(2) = \Delta E_{ij} = n_i \left[\frac{F(i,j)^2}{(\varepsilon_j - \varepsilon_i)}\right]$$

where n_i is the donor orbital occupancy, ε_i and ε_j are diagonal elements and F(i,j) is the off diagonal NBO Fock matrix element. These calculations allow us to analyze the probable charge-transfers and the intermolecular bond paths. ^{1}H and ^{13}C NMR chemical shifts are calculated with GIAO approach (Leena Sinha *et al*. 2013) by applying B3LYP/6-311++G (d, p) method and compared with the experimental NMR spectra.

The results indicate that the fundamental frequencies calculated (DFT) for the title compound show quite good agreement with experimental values. A small difference between experimental and calculated vibrational modes is observed. This discrepancy may be due to the formation of intermolecular hydrogen bonding. Also we note that the experimental results belong to solid phase and theoretical calculations belong to gaseous phase.

4. RESULT& DISCUSSION

4.1 Molecular geometry

The molecular structure of 2MBAP with C_1 symmetry is as shown in Fig 1.

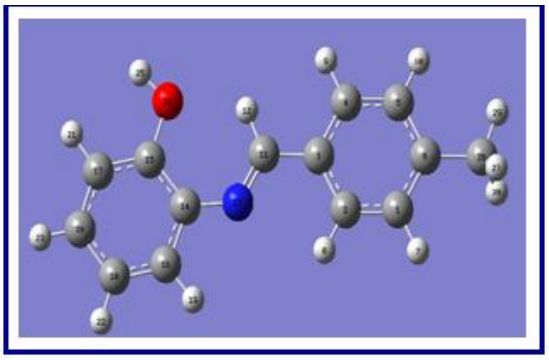

Fig. 1: The molecular structure of 2 MBAP with C_1 symmetry

Various theoretically computed energies, rotational constants and dipole moment are shown in Table 1.

Table 1. Various theoretically computed energies, rotational constants and dipole moment

Parameters	DFT (LanL2DZ)
Global minimum energy (a.u)	-671.1508
Zero point vibrational energy (Kcal/mol)	147.81235
Total energy (Kcal/mol)	156.602
Translational energy (Kcal/mol)	0.889
Rotational energy (Kcal/mol)	0.889
Vibrational energy(Kcal/mol)	154.82
Rotational constants (GHZ)	1.80761 0.20421 0.18370
Dipole moment (Debye)	2.1569

Table 2. Optimized geometrical parameters of 2MBAP

Bond length in (Á)		Bond angle in (°)		Dihedral angle in (°)	
C_1-C_2	1.3994	C_2-C_1-C_6	121.2277	C_6-C_1-C_2-C_3	0.0033
C_1-C_6	1.4183	C_2-C_1-H_7	119.6288	C_6-C_1-C_2-H_8	179.9975
C_1-H_7	1.089	C_6-C_1-H_7	119.1435	H_7-C_1-C_2-C_3	-179.9941
C_2-C_3	1.4178	C_1-C_2-C_3	120.4602	H_7-C_1-C_2-H_8	0.0001
C_2- H_8	1.0859	C_1-C_2-H_8	121.4205	C_2-C_1-C_6-C_5	-0.0087
C_3-C_4	1.4135	C_3-C_2-H_8	118.1193	C_2-C_1-C_6-C_{26}	179.9652
C_3-C_{11}	1.4728	C_2-C_3-C_4	118.5158	H_7-C_1-C_6-C_5	179.9887
C_4-C_5	1.4062	C_2-C_3-C_{11}	122.0229	H_7-C_1-C_6-C_{26}	-0.0373
C_4-H_9	1.0891	C_4-C_3-C_{11}	119.4613	C_1-C_2-C_3-C_4	0.0017
C_5-C_6	1.4111	C_3-C_4-C_5	120.771	C_1-C_2-C_3-C_{11}	179.9971
C_5-H_{10}	1.0882	C_3-C_4-H_9	119.4223	H_8-C_2-C_3-C_4	-179.9927
C_6-$C2_6$	1.5176	C_5-C_4-H_9	119.8067	H_8-C_2-C_3-C_{11}	0.0027
C_{11}-H_{12}	1.0922	C_4-C_5-C_6	120.8723	C_2-C_3-C_4-C_5	-0.0011
C_{11}-N_{13}	1.3043	C_4-C_5-H_{10}	119.6804	C_2-C_3-C_4-H_9	179.9927
N_{13}-C_{14}	1.4134	C_6-C_5-H_{10}	119.4473	C_{11}-C_3-C_4-C_5	-179.9967
C_{14}-C_{15}	1.4269	C_1-C_6-C_5	118.153	C_{11}-C_3-C_4-H_9	-0.0028
C_{14}-C_{16}	1.4177	C_1-C_6-C_{26}	120.5695	C_2-C_3-C_{11}-H_{12}	179.9996
C_{15}-C_{17}	1.4066	C_5-C_6-C_{26}	121.2775	C_2-C_3-C_{11}-N_{13}	0.0007
C_{15}-O_{24}	1.4048	C_3-C_{11}-H_{12}	116.2989	C_4-C_3-C_{11}-H_{12}	-0.005
C_{16}-C_{18}	1.4026	C_3-C_{11}-N_{13}	120.8682	C_4-C_3-C_{11}-N_{13}	179.9961
C_{16}-H_{19}	1.0859	H_{12}-C_{11}-N_{13}	122.8329	C_3-C_4-C_5-C_6	-0.0045
C_{17}-C_{20}	1.4056	C_{11}-N_{13}-C_{14}	126.0122	C_3-C_4-C_5-H_{10}	179.9952
C_{17}-H_{21}	1.0902	N_{13}-C_{14}-C_{15}	128.1994	H_9-C_4-C_5-C_6	-179.9983
C_{18}-C_{20}	1.4082	N_{13}-C_{14}-C_{16}	114.9856	C_3-C_4-C_5-H_{10}	0.0014
C_{18}-H_{22}	1.0864	C_{15}-C_{14}-C_{16}	116.815	C_4-C_5-C_6-C_1	0.0092
C_{20}-H_{23}	1.0869	C_{14}-C_{15}-C_{17}	121.1166	C_4-C_5-C_6-C_{26}	-179.9645
O_{24}-H_{25}	0.9793	C_{14}-C_{15}-O_{24}	118.3581	H_{10}-C_5-C_6-C_1	-179.9904
C_{26}-H_{27}	1.0988	C_{17}-C_{15}-O_{24}	120.5253	H_{10}-C_5-C_6-C_{26}	0.0358
C_{26}-H_{28}	1.0987	C_{14}-C_{16}-C_{18}	122.4407	C_1-C_6-C_{26}-H_{27}	-60.0838
C_{26}-H_{29}	1.0958	C_{14}-C_{16}-H_{19}	116.3146	C_1-C_6-C_{26}-H_{28}	59.195
		C_{18}-C_{16}-H_{19}	121.2448	C_1-C_6-C_{26}-H_{29}	179.5706
		C_{15}-C_{17}-C_{20}	120.4853	C_5-C_6-C_{26}-H_{27}	119.8893
		C_{15}-C_{17}-H_{21}	119.4961	C_5-C_6-C_{26}-H_{28}	-120.8319
		C_{20}-C_{17}-H_{21}	120.0186	C_5-C_6-C_{26}-H_{29}	-0.4563
		C_{16}-C_{18}-C_{20}	119.522	C_3-C_{11}-N_{13}-C_{14}	179.9979
		C_{16}-C_{18}-H_{22}	120.1402	H_{12}-C_{11}-N_{13}-C_{14}	-0.0009
		C_{20}-C_{18}-H_{22}	120.3378	C_{11}-N_{13}-C_{14}-C_{15}	-0.0055
		C_{17}-C_{20}-C_{18}	119.6204	C_{11}-N_{13}-C_{14}-C_{16}	179.9941
		C_{17}-C_{20}-H_{23}	119.7797	N_{13}-C_{14}-C_{15}-C_{17}	179.9998
		C_{18}-C_{20}-H_{23}	120.5999	N_{13}-C_{14}-C_{15}-O_{24}	0.0001
		C_{15}-O_{24}-H_{25}	111.6319	C_{16}-C_{14}-C_{15}-C_{17}	0.0003
		C_6-$C2_6$-H_{27}	111.213	C_{16}-C_{14}-C_{15}-O_{24}	-179.9995
		C_6-C_{26}-H_{28}	111.2256	N_{13}-C_{14}-C_{16}-C_{18}	179.9999
		C_6-C_{26}-H_{29}	111.4811	N_{13}-C_{14}-C_{16}-H_{19}	-0.0001

Continued: Table 2. Optimized geometrical parameters of 2MBAP

		H_{27}-C_{26}-H_{28}	107.0972	C_{15}-C_{14}-C_{16}-C_{18}	-0.0004
		H_{27}-C_{26}-H_{29}	107.8042	C_{15}-C_{14}-C_{16}-H_{19}	179.9995
		H_{28}-C_{26}-H_{29}	107.821	C_{14}-C_{15}-C_{17}-C_{20}	0.0
				C_{14}-C_{15}-C_{17}-H_{21}	180.0
				O_{24}-C_{15}-C_{17}-C_{20}	179.9998
				O_{24}-C_{15}-C_{17}-H_{21}	-0.0003
				C_{14}-C_{15}-O_{24}-H_{25}	-179.9991
				C_{17}-C_{15}-O_{24}-H_{25}	0.0012
				C_{14}-C_{16}-C_{18}-C_{20}	0.0003
				C_{14}-C_{16}-C_{18}-H_{22}	-179.9999
				H_{19},C_{16},C_{18},C_{20}	-179.9997
				H_{19},C_{16},C_{18},H_{22}	0.0001
				C_{15},C_{17},C_{20},C_{18}	-0.0002
				C_{15}-C_{17}-C_{20}-H_{23}	179.9998
				H_{21}-C_{17}-C_{20}-C_{18}	179.9998
				H_{21}-C_{17}-C_{20}-H_{23}	-0.0001
				C_{16}-C_{18}-C_{20}-C_{17}	0.0
				C_{16}-C_{18}-C_{20}-H_{23}	-180.0
				H_{22}-C_{18}-C_{20}-C_{17}	-179.9998
				H_{22}-C_{18}-C_{20}-H_{23}	0.0002

The most optimized structural parameters were also calculated and they were depicted in the Table 2.

In this work,The calculated geometrical parameters using DFT method consider only the gas phase, where the molecule is free of interactions.

4.2 Vibrational assignments

According to the theoretical calculations, the title molecule 2MBAP has 29 atoms and belongs to C_1 point group. It has 81 nrmal modes of vibrations. Out of this, there are 26 out of plane vibrations and 55 plane vibrations.

The detailed vibrtaional band assignments made on the title compound is presented in Table 3.

The below table indicates that the fundamental frequencies calculated (DFT) for the title Compound show quite good agreement with experimental values. A small difference between experimental and calculated vibrational modes is observed. This discrepancy may be due to the formation of intermolecular hydrogen bonding. Also we note that the experimental results belong to solid phase and theoretical calculations belong to gaseous phase.

For the visual comparison , the theoretical and experimental FT-IR spectra were reported in the fig. 2 and fig. 3 respectively. The assignments are based on the vibrational animations of fundamentals using the Gauss view package programme in the DFT/LanL2DZ calculations.

4.3 Vibrational analysis

In experimental method structure of the compound is assigned by comparing observed vibrational frequencies with the reported vibrational frequencies.

The absorption due to –OH, =C-O stretch of phenol are reported (Wolinski *et al.* 1997; Kalsi, 2004; Lever, 1968) in the region 3650 – 3200 cm^{-1} and 1300 -1000 cm^{-1} of the spectrum ·OH in plane bending and out of plane bending vibrations of phenols are reported (Rajanarendar *et al.* 2008; Silverstein and Webster, 1996) in the region 1420 – 1330 cm^{-1} and 765-650 cm^{-1} respectively. Band absorbed in the region 3367 cm^{-1}, 1380 cm^{-1}, (650,677,700) cm^{-1} and 1308 cm^{-1} are assigned to –OH stretching, OH in plane bending, OH out of plane bending and =C-O stretching vibrations of phenolic group of 2MBAP. C=N stretching vibrations of oximes, semi carbazones, thiosemicarbazones and hydrazones are reported in the 1690-1470 cm^{-1} region.

Table 3.

Mode Nos	Theoretical vibrational frequency (cm^{-1})		Experimental IR(cm^{-1})	Reduced Mass (amu)	Force constant (m dyne A^{-1})
	Unscaled	Scaled			
1	22.1017	21.12923	-	1.2540	0.0004
2	27.0922	25.90014	-	2.4013	0.0010
3	48.0907	45.97471	-	4.3639	0.0059
4	69.2131	66.16772	-	4.6807	0.0132
5	103.582	99.02401	-	4.4644	0.0282
6	184.898	176.7623	-	2.8701	0.0578
7	187.449	179.201	-	6.0501	0.1252
8	209.128	199.9268	-	4.8048	0.1238
9	260.745	249.2719	-	4.9550	0.1985
10	297.351	284.2679	-	2.6239	0.1367
11	340.244	325.2732	-	3.6258	0.2473
12	364.353	348.3212	-	4.0858	0.3196
13	373.768	357.3219	-	1.3162	0.1083
14	387.023	369.9935	-	3.9222	0.3461
15	427.739	408.918	410	2.8364	0.3058
16	480.283	459.1508	450	3.0846	0.4192
17	485.647	464.2782	462	5.7708	0.8019
18	528.495	505.2407	500	4.9659	0.8172
19	533.015	509.5622	510	2.6420	0.4422
20	573.151	547.9321	548	6.8654	1.3288
21	584.084	558.3846	550	3.5948	0.7226
22	638.713	610.6098	650	6.3867	1.5351
23	656.799	627.8995	677	6.9648	1.7702
24	745.698	712.8877	680	3.1409	1.0290
25	755.958	722.6958	700	5.4686	1.8413
26	763.996	730.3803	725	3.2062	1.1026
27	785.301	750.7479	740	1.2595	0.4576
28	787.277	752.6371	745	4.7650	1.7401
29	860.72	822.8482	810	5.6857	2.4818
30	861.511	823.604	820	1.3672	0.5979
31	883.263	844.3997	840	1.4753	0.6781
32	891.707	852.4715	870	5.4985	2.5759
33	892.947	853.6569	-	1.2752	0.5991
34	979.391	936.298	930	1.3644	0.7711
35	998.617	954.6777	950	1.3523	0.7946
36	1016.74	972.008	980	1.4309	0.8715
37	1022.72	977.723	982	1.3371	0.8240
38	1037.91	992.2444	990	1.3824	0.8774
39	1039.42	993.6825	-	2.8119	1.7899
40	1049	1002.839	1010	1.5885	1.0299
41	1059.59	1012.966	1020	2.2212	1.4693
42	1086.24	1038.447	1030	1.5655	1.0883
43	1104.69	1056.086	1040	2.2512	1.6187
44	1148.54	1098.005	1080	1.3756	1.0692
45	1177.49	1125.678	1118	1.2806	1.0461
46	1198.24	1145.515	1150	1.7703	1.4975
47	1203.32	1150.377	1153	1.3816	1.1787
48	1218	1164.407	-	1.2109	1.0584
49	1246.86	1192.002	1192	3.3175	3.0388

Continued: Table 3.

49	1246.86	1192.002	1192	3.3175	3.0388
50	1256.6	1201.306	1205	2.4863	2.3131
51	1287.16	1230.526	1220	2.4604	2.4017
52	1316.73	1258.798	1240	1.6342	1.6694
53	1349.18	1289.816	1298	1.3946	1.4956
54	1370.22	1309.93	1300	4.5203	5.0003
55	1380.63	1319.884	1310	4.6456	5.2174
56	1422.58	1359.982	1348	1.7116	2.0408
57	1444.06	1380.522	1380	1.3782	1.6933
58	1447.84	1384.134	1389	1.9199	2.3712
59	1481.45	1416.264	1428	2.2368	2.8923
60	1514.84	1448.185	1440	1.0470	1.4156
61	1518.58	1451.767	1450	1.1395	1.5483
62	1520.5	1453.598	1455	2.2917	3.1216
63	1549.06	1480.901	1480	2.7140	3.8370
64	1608.47	1537.694	1507	6.4029	9.7601
65	1620.91	1549.587	1510	6.1459	9.5138
66	1627.28	1555.679	1555	6.0745	9.4772
67	1658.45	1585.48	1580	6.1135	9.9071
68	1666.17	1592.856	1625	6.3279	10.3501
69	3034.55	2901.025	2870	1.0373	5.6277
70	3105.3	2968.669	2930	1.0981	6.2390
71	3137.06	2999.033	2900	1.0990	6.3724
72	3139.26	3001.136	3010	1.0885	6.3204
73	3172.95	3033.343	3030	1.0893	6.4611
74	3179.82	3039.91	3040	1.0875	6.4789
75	3185.55	3045.388	3042	1.0900	6.5167
76	3204.57	3063.57	3045	1.0963	6.6334
77	3205.42	3064.382	3050	1.0883	6.5882
78	3223.45	3081.619	2900	1.0941	6.6981
79	3232.05	3089.84	3000	1.0945	6.7361
80	3240.47	3097.888	3367	1.0991	6.8000
81	3696.97	3534.299	3500	1.0662	8.5854

Absorption noted in the region 1625 cm^{-1}, is assigned to C=N stretching vibration. Presence of phenyl group was provedby the absorptions 3010 cm^{-1} (aromatic C-H stretch) 1507 cm^{-1} (C=C of phenyl ring) 1030,1040,1080, 840 (in plane bending of phenyl ring) and 840 and 680 cm^{-1} (out of plane bending of phenyl gro up). Absorption band noted in the region 2930 and 2870 cm^{-1} is assigned -CH_3 Asymmetric and Symmetric stretching respectively.

4.4 Electronic absorption spectra and molecular orbitals

The theoretical electronic absorption spectra calculated on the TD-DFT/B3LYP/6-311 G(d,p) Method level optimized structure are listed in the table 4.

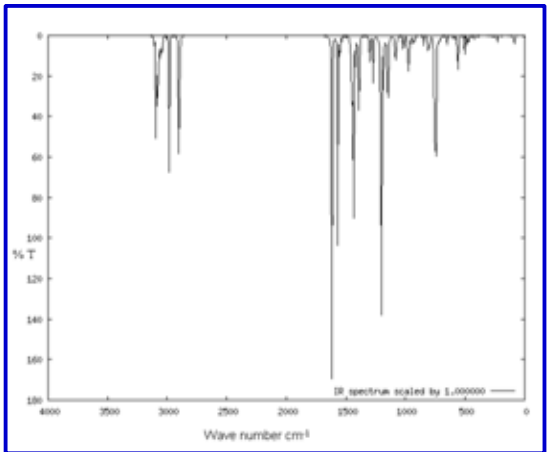

Fig. 2: Theoretical IR spectra

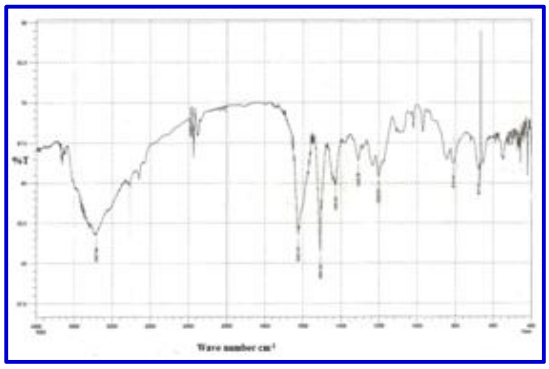

Fig. 3: Experimental FT-IR spectra of 2MBAP

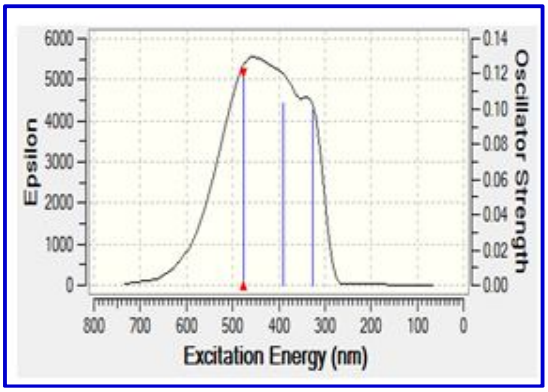

Fig. 4: Theoretical IR spectra

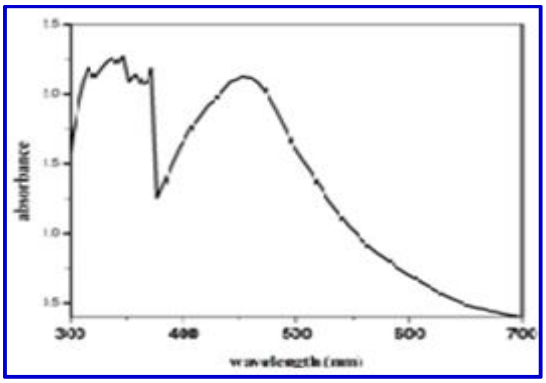

Fig. 5: Experimental FT-IR spectra

Table 4. Theoretical and Experimental Electronic absorption spectral data

Oscillator strength	Theoretical Wavelength λ_{max} (nm)	Experimental Wavelength λ_{max} (nm)
0.1204	475.64	469
0.1035	389.15	372
0.0991	325.84	330

The calculated results involving the vertical excitation energies, oscillator strength(f) and wavelength are carried out and compared with measured experimental wavelength. Typically, according to the Frank-Condon principle, the maximum absorption peak (λ_{max}) corresponds in an UV-Visible spectrum to vertical excitation.TD-DFT/ B3LYP predicts three electronic transitions which are in good agreement with the measured experimental values. For the title compound, $\pi \rightarrow \pi^*$ and $n \rightarrow \pi^*$ transitions are the most probable transitions.

Highest Occupied Molecular Orbital (HOMO) 56 and Lowest Unoccupied Molecular Orbital (LUMO) 57 for 2MBAP are very important parameters for quantum chemistry, and these orbitals are the main orbital taking part in electronic excitation and chemical reaction. Frontier molecular orbitals (HOMO & LUMO) may be used to predict the adsorption centers of the inhibitor molecule. For the simplest transfer of electrons, adsorption should occur at the part of the molecule where the softness, σ, a local property, has the highest value.

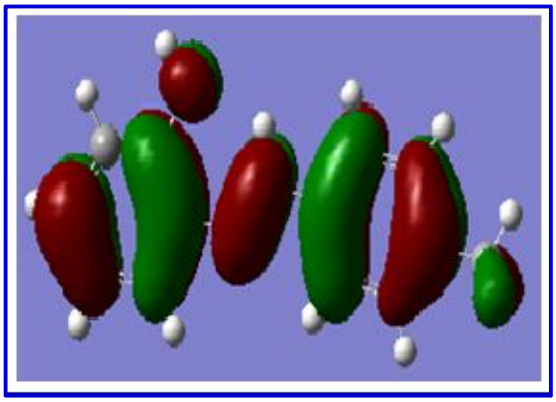

Fig. 6:HOMO

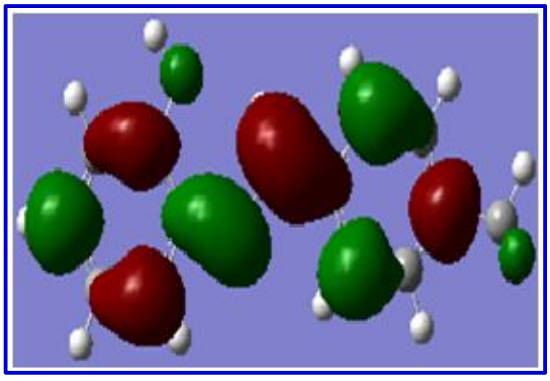

Fig. 7: LUMO

The HOMO, LUMO energies are used to describe the dynamic stability, hardness and softness of a molecule. According to Koopman's theorem (Awad, 2009), the energies of the HOMO and the LUMO orbitals of the inhibitor molecule are related to the ionization potential (IP), and the electron affinity (EA), by the following relations:

$E_{LUMO} = -|EA| = -0.09055$
$E_{HOMO} = -|IP| = -0.22504$

Where EA is the electron affinity and IP is the ionization potential. The hardness of the molecule is given by $\eta=(E_{LUMO} - E_{HOMO})/2 = 0.06725$. The softness is the reciprocal of hardness $\sigma = 1/\eta = 14.8710$. Here the value of softness is high. Therefore the inhibition efficiency of the title molecule 2MBAP is also high. Furthermore the calculated quantum chemical parameters show that the title molecule 2MBAP has lower separation energy, $\Delta E=0.13449$ a.u, between the HOMO level and the LUMO level. This leads to increase in its reactivity towards the metal surface and accordingly increases its inhibition efficiency. Moreover, lower the HOMO-LUMO energy gap explains the eventual charge transfer interaction taking place within the molecule. The atomic orbital compositions of the frontier molecular orbital for 2MBAP are sketched in fig. 6 and fig. 7. Here the positive phase is red and negative one is green.

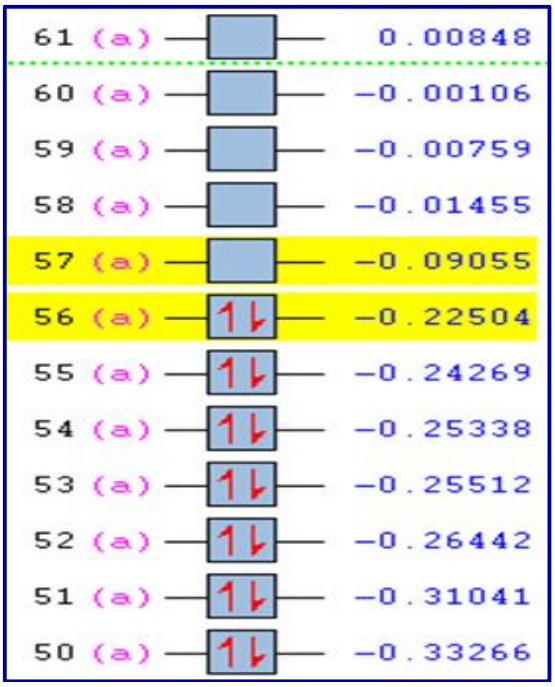

Fig. 8: Energy levels of 2 MBAP

4.5 Prediction of polarisability and first hyperpolarizability

The electronic dipolemoment (μ_{tot}), molecular polarizability (α_{tot}),anisotropy of polarizability ($\Delta\alpha$) andthe molecular first hyperpolarizability (β_{tot}) of the novel molecular system were investigated using B3LYP/ LanL2DZ method, based on the finite field approach (Awad, 2009) They are calculated using the following equations.

$\alpha_{tot} = 1/3(\alpha_{xx} + \alpha_{yy} + \alpha_{zz})$

$\Delta\alpha = 1/\sqrt{2}\{(\alpha_{xx} - \alpha_{yy})^2 + (\alpha_{yy} - \alpha_{zz})^2 + (\alpha_{zz} - \alpha_{xx})^2 + 6\alpha^2_{xz} + 6\alpha^2_{xy} + 6\alpha^2_{yz}\}^{1/2}$

$\beta = \{(\beta_{xxx} + \beta_{xyy} + \beta_{xzz})^2 + (\beta_{yyy} + \beta_{yzz} + \beta_{yxx})^2 + (\beta_{zzz} + \beta_{zxx} + \beta_{zyy})^2\}^{1/2}$

$\mu_{tot} = (\mu_x^2 + \mu_y^2 + \mu_z^2)$

$\beta_x = \beta_{xxx} + \beta_{xyy} + \beta_{xzz}$

$\beta_y = \beta_{yyy} + \beta_{yzz} + \beta_{yxx}$

$\beta_z = \beta_{zzz} + \beta_{zxx} + \beta_{zyy}$

Table 5. The Dipolemoment μ, The Polarizability α, Average polarizability α_{tot}, Anisotropy of polarizability Δα (esu) and the Molecular first hyperpolarizability β (esu) of the title molecule 2MBAP

μ_x	0.9646 (Debye)	β_{xxx}	1089.957633(a.u)
μ_y	-0.3266 (Debye)	β_{yxx}	32.061021(a.u)
μ_z	2.5244 (Debye)	β_{xyy}	3.7339655(a.u)
μ_{tot}	2.7221 (Debye)	β_{yyy}	-42.4247064(a.u)
α_{xx}	322.5134529(a.u)	β_{zxx}	-29.1778324(a.u)
α_{xy}	-18.4921697(a.u)	β_{zyy}	2.597112(a.u)
α_{yy}	161.0032553(a.u)	β_{xzz}	-3.2562108(a.u)
α_{xz}	-3.8077706(a.u)	β_{yzz}	-10.6635427(a.u)
α_{yz}	-11.0521772(a.u)	β_{zzz}	3.9745752(a.u)
α_{zz}	67.0139681(a.u)	β_x	1203294.496(a.u)
α_{tot}	2.7196×10^{-23}(esu)	β_y	7250.398199(a.u)
$\Delta\alpha$	3.3644×10^{-23}(esu)	β_z	1278.028152(a.u)
		β	$9.510385839\times10^{-30}$(esu)

The polarizability and the hyperpolarizability tensors can be obtained by a frequency job output file of Gaussian. However α and β values of Gaussian output are in atomic units (a.u). So they have been converted into electronic units (esu). It is well known that the higher values of dipole moment, molecular polarizability and hyperpolarizability than urea are important for more active NLO properties. For the title molecule 2MBAP, the value of dipolemoment, molecular polarizability and hyperpolarizability are very much

greater than those of urea. That is to say, the title compound can be a good candidate of NLO material.

4.6 NMR spectra

The isotropic chemical shifts are frequently used as an aid in identification of reactive organic as well ionic species. It is recognized that accurate predictions of molecular geometries are essential for reliable calculations of magnetic properties. Therefore, full geometry optimization of 2MBAP is performed by using B3LYP/6-311++G(d,p) level. Then ^{1}H and ^{13}C NMR chemical shifts are calculated by GIAO, method applying B3LYP /6-311++G(d,p) levels. GIAO procedure is somewhat superior since it exhibits a faster convergence of the calculated properties upon extension of the basis set used. On the other hand, the density functional methodologies offer an effective alternative to the conventional methods, due to their significantly lower computational cost. In table 6, the theoretical ^{1}H and ^{13}C isotropic chemical shifts (with respect to TMS, all values in ppm) for the title compound are given. As can be seen from Table 6, theoretical ^{1}H and ^{13}C chemical shift results of the title compound are generally closer to the literature ^{1}H and ^{13}Cchemical shift data.

C-11 is attached with electron with-drawing N-13 atom. Here N-13 decrease the shielding and move the resonance of C-11 towards a higher frequency (171.4401 ppm). C-26 is an aliphatic carbon .But it comes to resonance at somewhat higher frequency (23.293ppm) than the expected (15 ppm) since it is attached with phenyl ring

Table 6.

Atom position	B3LYP/6-311++G(d,p)	Atom position	B3LYP/6-311++G(d,p)
H_{12}	10.1885	C_{11}	171.4401
H_8	8.9743	C_{15}	163.1139
H_{19}	7.9482	C_6	151.3372
$H_{9,7}$	7.6246	C_3	145.5069
H_{10}	7.502	C_{14}	145.269
$H_{22,23}$	7.2665	C_{16}	142.752
H_{21}	6.7093	C_4	140.2444
H_{25}	4.5857	C1	136.5776
$H_{27,28}$	2.73835	C_5	136.3242
H_{29}	2.0613	C_{20}	134.1804
		C_2	134.0054
		C_{18}	129.1252
		C17	121.2733
		C_{26}	23.293

4.7 NBO analysis

Second order perturbation theory analysis of fock matrix in NBO basis for 2MBAP is shown in table 7.

The NBO analysis offers a handy basis for exploring charge transfer or conjugative interaction in molecular systems and is an efficient method for studying intra - and intermolecular bonding and interaction among bonds (Awad, 2009; Amal Raj, 2006; Liu Jun-na, 2005) A summary of electron donor orbitals, acceptor orbitals and the stabilization energies larger than 3 Kcal/mol that resulted from the second-order perturbation theory are reported in table 7.

The intramolecular hyperconjugative interactions are formed by the orbital overlap between σ(C-C)→ σ^* (C-C), π (C-C) → π^* (C-C) and bond orbitals, which results in ICT (Intra molecular charge transfer)causing stabilization of the system. The larger the E(2) value, the stronger is the interaction between electron donors and electron acceptors, reflects a more donating tendency from electron donors to electron acceptors and a greater degree of conjugation of the whole system.

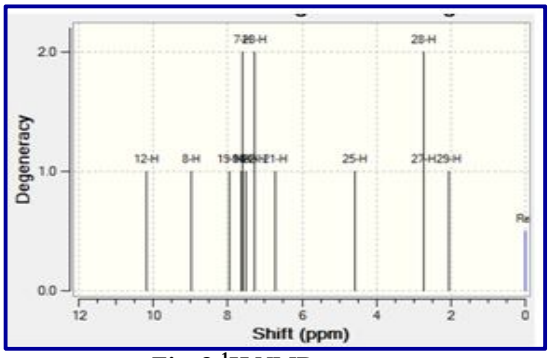

Fig. 9:^{1}H NMR spectra

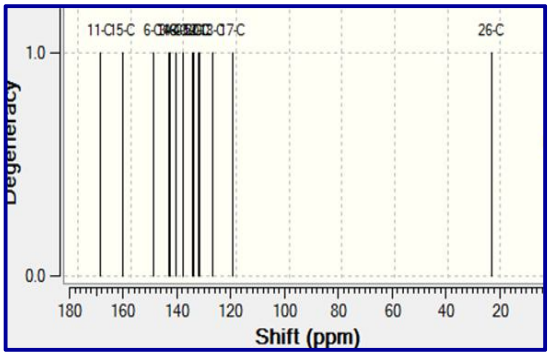

Fig. 10:^{13}C NMR spectra

Table 7.

Donar	Type	Occupancy (a.u)	Acceptor	Type	Occupancy (a.u)	$E^{(2)}$ Kcal/mol	$E_j - E_i$ (a.u)	F (a.u)
C_1-C_2	σ	1.97823	C_3-C_{11}	σ^*	0.03161	4.32	1.16	0.063
C_1-C_2	σ	1.97823	C_6-C_{26}	σ^*	0.01688	4.22	1.07	0.060
C_1-C_2	π	1.67742	C_3-C_4	π^*	0.37640	19.64	0.28	0.067
C_1-C_2	π	1.67742	C_5-C_6	π^*	0.33846	23.05	0.28	0.072
C_1-C_6	σ	1.97497	C_5-H_{10}	σ^*	0.01599	3.25	1.18	0.055
C_1-H_7	σ	1.97711	C_2-C_3	σ^*	0.02722	5.26	1.05	0.066
C_1-H_7	σ	1.97711	C_5-C_6	σ^*	0.02545	5.67	1.06	0.069
C_2-C_3	σ	1.97302	C_1-H_7	σ^*	0.01620	3.09	1.17	0.054
C_2-C_3	σ	1.97302	C_4-H_9	σ^*	0.01589	3.14	1.17	0.054
C_2-H_8	σ	1.97579	C_1-C_6	σ^*	0.02647	5.41	1.04	0.067
C_2-H_8	σ	1.97579	C_3-C_4	σ^*	0.02288	5.78	1.04	0.069
C_3-C_4	π	1.63049	C_1-C_2	π^*	0.27805	20.03	0.28	0.069
C_3-C_4	π	1.63049	C_5-C_6	π^*	0.33846	19.78	0.28	0.067
C_3-C_4	π	1.63049	C_{11}-N_{13}	π^*	0.17570	20.03	0.28	0.069
C_3-C_{11}	σ	1.96845	C_4-C_5	σ^*	0.01351	3.48	1.19	0.057
C_3-C_{11}	σ	1.96845	N_{13}-C_{14}	σ^*	0.02553	6.61	1.06	0.075
C4-C_5	σ	1.97773	C_3-C_{11}	σ^*	0.03161	4.12	1.16	0.062
C_4-C_5	σ	1.97773	C_6-C_{26}	σ^*	0.01688	4.41	1.07	0.061
C_4-H_9	σ	1.97720	C_2-C_3	σ^*	0.02722	5.65	1.05	0.069
C_4-H_9	σ	1.97720	C_5-C_6	σ^*	0.02545	5.17	1.06	0.066
C_5-C_6	σ	1.97546	C_1-H_7	σ^*	0.01620	3.13	1.19	0.055
C_5-C_6	π	1.64678	C_1-C_2	π^*	0.27805	17.63	0.29	0.065
C_5-C_6	π	1.64678	C_3-C_4	π^*	0.27805	22.94	0.28	0.072
C_5-H_{10}	σ	1.97761	C_1-C_6	σ^*	0.02647	5.64	1.05	0.069
C_5-H_{10}	σ	1.97761	C_3-C_4	σ^*	0.02288	5.11	1.05	0.066
C_6-C_{26}	σ	1.9802	C_1-C_2	σ^*	0.01311	3.52	1.18	0.058
C_6-C_{26}	σ	1.9802	C_4-C_5	σ^*	0.01351	3.60	1.17	0.058
C_{11}-H_{12}	σ	1.98203	C_2-C_3	σ^*	0.02722	5.58	1.06	0.069
C_{11}-N_{13}	π	1.88519	C_3-C_4	π^*	0.27805	9.78	0.35	0.056
C_{11}-N_{13}	π	1.88519	C_{14}-C_{16}	π^*	0.38067	14.38	0.34	0.067
N_{13}	LP(1)	1.91725	C_{11}-H_{12}	σ^*	0.03585	11.73	0.79	0.087
N_{13}	LP(1)	1.91725	C_{14}-C_{15}	σ^*	0.04749	12.27	0.81	0.90
O_{24}	LP(2)	1.88807	C_{15}-C_{17}	σ^*	0.02398	23.63	0.35	0.087
C_{11}-N_{13}	π^*	0.17570	C_3-C_4	π^*	0.27805	78.14	0.02	0.068
C_{11}-N_{13}	π^*	0.17570	C_{14}-C_{16}	π^*	0.38067	96.48	0.01	0.057
C_{15}-C_{17}	π^*	0.38934	C_{14}-C_{16}	π^*	0.38067	191.58	0.02	0.081
C_{15}-C_{17}	π^*	0.38934	C_{18}-C_{20}	π^*	0.35587	214.25	0.02	0.081

E(2) means energy of hyperconjugative interactions (stabilization energy).
$E_j - E_i$ Energy difference between donor and acceptor i and j NBO orbitals.
F(i, j) is the Fock matrix element between i and j NBO orbitals.

The strong intramolecular hyperconjugative interactions of the σ and π electrons of C-C to the anti C-C bond of the aromatic rings results to stabilization of some part of the rings as evident from table 5. The intramolecular hyperconjugative interactions of the $\sigma(C_1\text{-}C_2)$ distributes to$\sigma^*(C_3\text{-}C_{11})$ leading to stabilization of 4.32 Kcal/mol. This enhances further conjugation with antibonding orbital of $\sigma^*(C_6\text{-}C_{26})$, $\pi^*(C_3\text{-}C_4)$ and $\pi^*(C_5\text{-}C_6)$ which results to strong delocalization of 4.22,19.64 and 23.05 Kcal/mol, respectively. The same kind of interaction is calculated in the other bonds as shown in table. The most important interaction energies of N_{13} LP(1) → σ^* (C_{11}-H_{12}), N_{13} LP(1) → σ^* (C_{14}-C_{15}) and O_{24} LP(2) → σ^* (C_{15}-C_{17}) are 11.73,12.27 and 23.63 Kcal/mol, respectively. π^* (C_{15}-C_{17}) → π^* (C_{18}-C_{20}) gives the strongest stabilization energy (214.25 Kcal/mol) to the system.

5. CONCLUSION

Density functional theory calculations have been carried out to determine the electronic absorptions, vibrational frequencies, H^1 NMR and ^{13}CNMR chemical shifts.IR and UV data alone are compared with the experimental values . The theoretically computed scaled wave numbers calculated by computational method are found to be in reasonably good agreement with that obtained in the experimental FT-IR and UV spectrum of the 2MBAP. From the study, we conclude that the title compound 2MBAP have higher inhibition efficiency and also posses better NLO properties. The stability and intramolecular interactions have been interpreted by NBO/NLO analysis and the transactions give stabilization to the structure have been identified by second order perturbation energy calculations.

ACKNOWLEDGEMENT

We are thankful to Sri Sarada College for Women, (Autonomous), Salem-16 for providing laboratory and computational facilities.

REFERENCES

Amal Raj, Rehunathan, R., Hubert Joe, I., Jayakumar, V. S., Structural conformation and vibrational spectroscopic studies of 2,6-bis (p-N,N-dimethyl benzylidene) cyclo hexanone using density functional theory, *J. Raman Spectrosc.*, 37, 1381(2006) . doi:10.1002/jrs.1554

Awad, M. K., Issa, R. M. and Atlam, F. M., Theoritical investigation of th inhibition of corrosion bysome triazole Schiff bases, *Materials and Corrosion*, 10(60), 9999(2009) .

De, B. and Ramasarma, G. S., Determination of pKaand correlation with the analgesic activity of 5-oximidazolylaminompyrazole 4-carboxaldehydes and their schiff bases Indian drugs, 36,583(1999).

Dhar, D. N. and Taploo, C. L., Schiff bases and their applications, *J. Sci. Ind. Res.*, 41, 501(1982).

Dyer John R., Applications of absorption spectroscopy of organic compounds, Prentice-Hall of India Limited, New Delhi, 5, 33(1984).

Essoufi, H., Kertit, S., Hammouti, B., Benkaddour M., 1-phenyl-5-mercapto-1,2,3,4 tetrazole as corrosion inhibitor of Nickel in sulphuric acid solution, *Bull. Electrochem.*, 16, 205-208(2000)

Gupta, V. K ., Singh, A. K ., Gupta, B., A cerium(III) selective polyvinyl chloride membrane sensor based on a Schiff base complex of N,N′-bis[2-(salicylideneamino)ethyl]ethane-1,2-diamine, *Anal.chem.Acta.*, 575,198(2006).

Hadjipavlu, L., Dimitra, J., Geronikaki and Athina, A., Thiazolyl and benzothiazolyl Schiff basesas novelpossible lipoxygenase inhibitors and anti-inflammatory agents, *Drug Des. Discov.*, 15, 199(1998).

Kertit, S. and Hammouti, B., 1-phenyl-5-mercapto-1,2,3,4-tetrazole as corrosion inhibitor of Iron in 1M HCl, *Appl. Surf. Sci.*, 93, 59(1996).

Kertit, S., Essoufi, H., Hammouti, B., Benkaddour, M., 1-phenyl-5-mercapto-1,2,3,4-tetrazole, A novel corrosion inhibitor of copper-zinc alloy which is very effective in low concentration, *J. Chem. Phys.*, 95, 2072(1998).

Kalsi, P. S., Spectroscopy of organic compounds, New Age International publishers, 6th edn., 132(2004).

Leena Sinha, Mehmet Karabacak, Narayan, V., Mehmet Cinar, Onkar Prasad, Molecular structure,electronic properties, NLO, NBO analysis and spectroscopic characterization of Gapapentin with experimental (FT-IR and Raman) techniques and quantum chemical calculations Spectrochimica Acta Part A: Molecular and Biomolecular Spectroscopy, 109, 298– 307(2013). doi:10.1016/j.saa,2013.02.035

Lever, A. B. P., Inorganic Electronic Spectroscopy, Elsevier, Newyork, 1968.

Liu Jun-na, Chen Zhi-rang, Yuan Shen-fang, Study on the prediction of visibleabsorption maxima of azobenzene compounds, *J. Zhejiang Univ. Sci.*, 6B,584(2005) . doi:10.1631/JZUS.2005.130584

Luo, X., Zhao, J., Ling, Y. and Liu, Z., Antioxidative effect of Schiff bases witho-hydroxy benzilidene group on free radical induced hemolysis of human red blood cell., *Chem. Abstr.*, 138, 247(2003).

Nishinaga, A., Yamada, T., Fujisawa, H. and Ishizaki K., Catalysis by cobalt schiff base complexes in the oxygenation of alkenes on the mechanism of ketonization, *J. Mol. Catal*., 48, 249-264(1988).

Parr, R. G. and Yang, W., Density- functional theory of atoms and molecules, Oxford University Press, Oxford, (1989).

Rajanarendar, E., Pashoshaik Firoz and Sivarama Reddy A. A, Simplified calogan's approach to synthesis of new isooxazolyl indazoles Indian, *J. Chem.*, 47B, 1591-1596(2008).

Sastri, V. S., Perumareddi, J. R., Molecular orbital theoretical studies of some organic corrosion inhibitors, *Corrosion*, 53, 671(1997).

Shemiran,i F., Mirroshandel, A. A., Salavati-Niasari M. and Kozari, R. R, Silica gel coated with Schiff bases: Synthesis and application as an adsorbant for cadmium, copper, zinc and nickel determination after preconcentration by Flame atomic absorption spectroscopy, *J. Anal. Chem*., 59,228 (2004).
doi:10.1023/b:JANC.0000018964.411166.

Silverstein Robert M., Francis and Webster, S., Spectrometric identification of organic compounds, John Wiley and sons, Inc Newyork, 6th edn., 36,81-90(1996),

Wolinski, K., Haacke, R., Hinton, J. F. and Pulay, P., Methods for parallel computation of SCF, NMR chemical shifts by GIAO method, *J. Comp. Chem.*, 18(6), 816–825(1997).
doi:10.102/(SICI)1096-987(1997043)1

Yan, C. W., Lin, H. C. and Cao, C. N., Investigation of inhibition of 2-mercaptobenzooxazoleb for copper corrosion, *Electrochim. Acta*., 45, 2815 (2000).
doi:10.1016/SOO13-4686(00)00385-6

Zucchi, F., Trabanelli, G. and Fonsati, M., Tetrazole derivatives as corrosion inhibitors for copper in copper chloride solutions, *Corros. Sci*., 38, 2019-2029(1996).
doi:10.1016/s0010-938(96)00094-7.